ISBN: 978-3-95450-253-0 ISSN: 2673-5571 doi:10.18429/JACoW-HB2023-TUA3I4

SARAF MEBT COMMISSIONING

N. Pichoff†, J. Dumas, A. Chance, F. Gougnaud, F. Senée, D. Uriot
Commissariat à l'énergie atomique et aux énergies alternatives, Gif-Sur-Yvette, France
A. Kreisel, Y. Luner, A. Perry, E. Reinfeld, R. Weiss-Babai, L. Weissman
Soreq Nuclear Research Center, Yavne, Israel

Abstract

SNRC in Israel is in the process of constructing a neutron production accelerator facility called SARAF. The facility will utilize a linac to accelerate a 5 mA CW deuteron and proton beam up to 40 MeV. In the first phase of the project, SNRC completed construction and operation of a linac (referred to as SARAF Phase I) which included an ECR ion source, a Low-Energy Beam Transport (LEBT) line, and a 4-rod RFQ. The second phase of the project involves collaboration between SNRC and Irfu in France to manufacture the linac. The injector control system has been updated and the Medium Energy Beam Transport (MEBT) line has been installed and integrated into the infrastructure. Recent testing and commissioning of the injector and MEBT with 5 mA CW protons and 5 mA pulsed Deuterons, completed in 2022 and 2023, will be presented and discussed. A special attention will be paid to the experimental data processing with the Bayesian inference of the parameters of a digital twin.

INTRODUCTION

The SARAF-Linac [1] is presented. The 5 mA proton or deuteron beam is bunched with a 176 MHz four-rods RFQ (~4 m) and accelerated with a superconducting linac consisting in 27 HWR and 20 Solenoids in four cryomodules (~5 m each).

Between the RFQ and the superconducting linac, the 5 m Medium Energy Beam Transport (MEBT) section consists of 3 rebunchers and 8 quadrupoles, each equipped with a steerer for orbit correction. The MEBT serves various purposes, including matching the beam from the RFQ to the Linac, minimizing the residual gas sent to the Superconducting Linac (SCL), characterizing beam properties such as current, position, phase, energy, transverse and longitudinal profiles, and emittances and, if needed, shape the beam using three sets of slits and a fast chopper (which will be installed at a later date).

The MEBT was initially constructed and tested at CEA Saclay during the first half of 2020. A dedicated test stand was utilized to ensure proper alignment, vacuum, cooling, power supplies, and associated control systems. Subsequently, the MEBT was transported to Israel in August 2020 to be installed and integrated by SNRC teams in its final position downstream the RFQ. The MEBT commissioning was conducted in parallel with other activities. Interceptive diagnostics are placed in 2 Diagnostics Boxes called DB1 at the middle of the MEBT and DB2 at the end of the MEBT.

Figure 1 shows the MEBT layout enhancing beam diagnostics:

- two ACCTs (ACCT2 and ACCT3) for current monitoring, transmission, and machine protection,
- one Faraday Cup (FC) in DB2 to stop the beam and measure its current,
- four BPMs to measure beam average positions and phase,
- one Fast Faraday Cup (FFC) in DB1 to measure the bunch length,
- one Wire Scanner (WS) in DB1 to measure the beam transverse profiles,
- one SEM-Grid (SG) in DB2 to measure the beam transverse profiles.

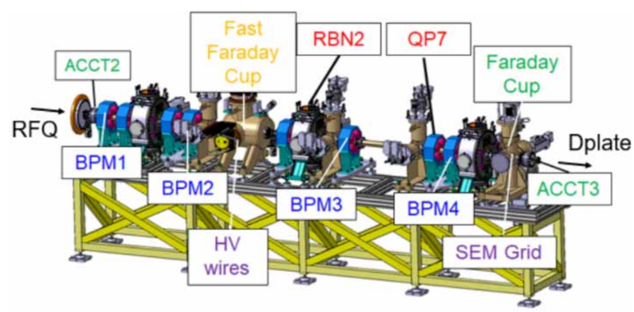

Figure 1: Layout of the MEBT, the 8 quadrupoles (QP) are in blue, the 3 rebunchers (RBN) are in light grey, and beam diagnostics are specifically shown.

For the MEBT commissioning, a D-plate previously employed during Phase I was connected downstream the MEBT. Figure 2 shows available beam diagnostics in the D-plate such as phase probes, FFC, MPCT (for current monitoring) and a set of slits and wires for transverse emittance measurements.

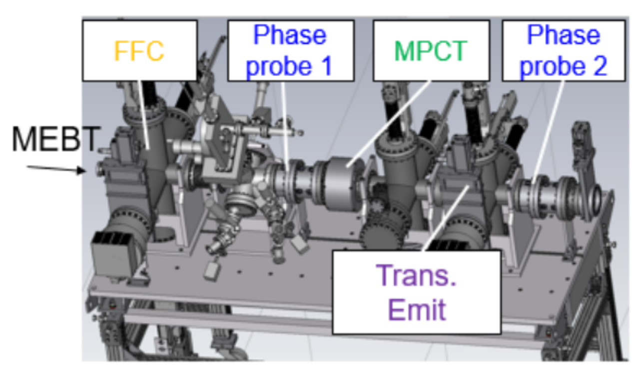

Figure 2: D-plate beam diagnostics [2].

ISBN: 978-3-95450-253-0 ISSN: 2673-5571 doi:10.18429/JACoW-HB2023-TUA3I4

LINAC TUNING

EIS Tuning

The observation of the beam position in BPM1 (Fig. 3) shows that, despite a nominal current reached in about 5 minutes, the beam moves during at least 20 minutes after the switch ON of the EIS (ECR Ion Source) start.

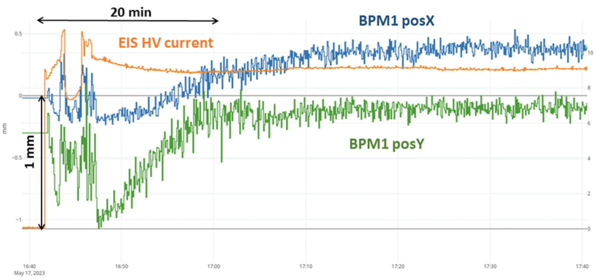

Figure 3: Beam position evolution in BPM1 after the EIS start.

The EIS voltage has been tuned by maximizing the RFQ transmission measured with ACCT2 (Fig. 4).

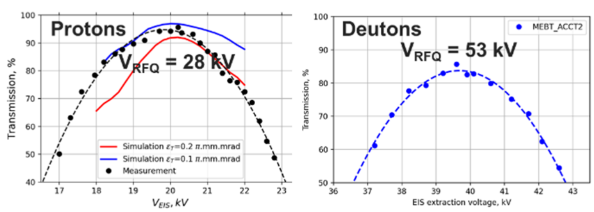

Figure 4: RFQ transmission as a function of the EIS voltage for protons (left) and deuterons (right).

RFQ Tuning

Using the new LLRF hardware and software, the required voltages for proton operation were applied to the RFQ and rebunchers. The EIS voltage and LEBT optics were adjusted to maximize beam transmission at the RFQ exit. Beam current was measured at different locations, including the LEBT's ACCT1, and MEBT's ACCT2 and FC. Figure 5 shows that the RFQ transmission plateau (over 90%) is reached at 710 mV, corresponding to a vane voltage of 28 kV.

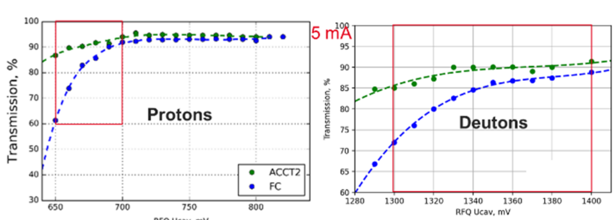

Figure 5: Proton (left) and deuteron (right) beam transmissions from RFQ input to MEBT ACCT2 (green), and FC (blue), as a function of the LLRF Uamp (RFQ voltage).

The MEBT optics were set according to beam dynamics simulations. The measurements demonstrated almost 100% MEBT transmission at nominal RFQ voltage.

Rebuncher Phasing

The three RBN were tuned using the Signature Matching method [3] with 2 downstream BPMs (in MEBT for RBN1&2 and in D-plate for RBN3). The data obtained from the measurement was well-matched with a cosine fit and TraceWin simulations (Fig. 6).

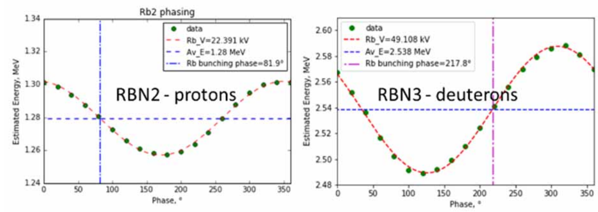

Figure 6: RBN phasing. In green is the estimated energy based on the measurement of the phase difference between BPMs. In red is the cosine fit. Left: RBN2 with protons; Right: RBN3 with deuterons.

BEAM CHARACTERIZATION

Transverse Sizes and Emittances

Three devices can be used to measure the beam transverse size: a wire scanner in DB1, a SEM-Grid in DB2 and another wire scanner in the D-plate.

The transverse emittances and the beam Twiss parameters at the exit of the RFQ can be deduced with TraceWin code [4] from the measurement of the beam sizes with varying upstream quadrupole strength (Fig. 7).

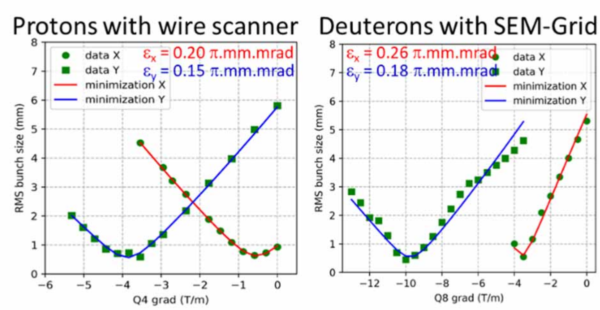

Figure 7: Beam RMS sizes as a function of a quadrupole gradients for protons in DB1 (left) and deuterons in DB2 (right). Beam emittance are deduced.

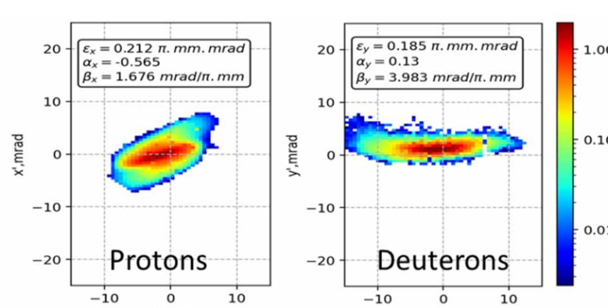

Figure 8: Transverse phase-space distribution from the emittance meter in the D-Plate for protons (left) and deuterons (right).

ISBN: 978-3-95450-253-0 ISSN: 2673-5571 doi:10.18429/JACoW-HB2023-TUA3I4

The beam distribution in transverse sub-phase-spaces can also be measured in the D-plate with a set of slits coupled with wires (Fig. 8). The emittances measured with the 2 technics are consistent, but may sometime differ up to 30% in certain conditions.

Longitudinal Size and Emittance

The Fast Faraday Cup is used to measure the longitudinal bunch profile in DB1 or in the D-plate. The longitudinal emittance and the beam Twiss parameters at the exit of the RFQ can be deduced with TraceWin code from the measurement of the bunch length with varying upstream rebuncher voltages (Fig. 9). For this measurement, a 6 GHz bandwidth scope located close to the FFC were used.

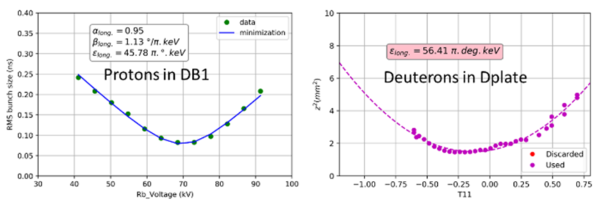

Figure 9: Longitudinal bunch size measured on the FFC as a function of the upstream rebuncher voltage for protons in DB1 (left) and deuterons in D-plate (right).

The reconstructed beam distribution fits with margins in the linac longitudinal acceptance (Fig. 10).

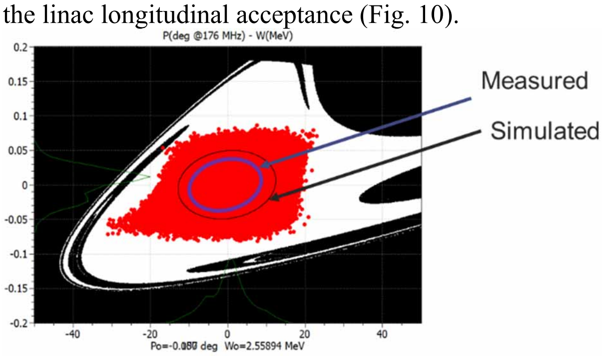

Figure 10: Measured beam in linac acceptance.

High Power Proton Beam Test

The 5 mA proton beam power has been ramped-up to 97.5% duty-cycle with a repetition rate of 10Hz. The beam has then been operated during 15 hours. 15 beam trips (from RFQ and Protection Systems) represented in blue on Fig. 11 occurred. Some investigations will be required in the future in order to reach higher availability.

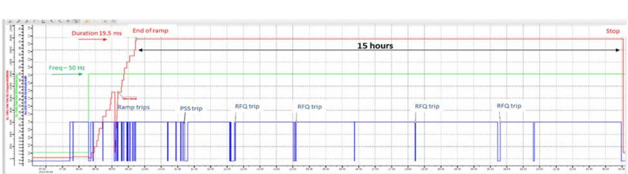

Figure 11: Ramping up of duty cycle for the proton beam in the MEBT. Pulse length in red (in µs), pulse frequency in green (in Hz) and beam presence in the beamline in blue.

We took the decision not to ramp-up the deuteron beam duty-cycle in order to preserve the RF amplifier of the RFQ (no spare available now).

Much more details on the MEBT commissioning results can be found in Ref. [5].

MACHINE LEARNING

Digital Twin (DT)

As seen in preceding paragraphs, the usual way to process experimental measurements is to extract beam deduced properties (emittances, Twiss parameters…) from beam measured properties (sizes, lengths, phases…) in different controlled conditions (varying quadrupole strengths or rebuncher phases or voltages…).

Nevertheless:

- The reconstructed properties are not exactly those of the real beam, due to measurement or reconstruction errors/uncertainties.
- Only a part of the beam properties at a specific position can be accessed at the same time.
- The measurements correspond to specific experimental conditions (particle type, current, machine tuning), which can be different from the final conditions.
- The use of these measurement results to do predictions with associated uncertainties are then not straightforward.

In order to improve the use of these experimental results, we propose to define and use a Digital Twin (DT) of the machine.

- In real world, the linac is operated according to physical and control parameters.
  For example: Qpole Power supply currents, *QP_I*.
- In virtual world, the linac is modelled by the DT made of the TraceWin simulation toots (modelling physical parameters) using a linac description with model parameters (modelling control parameters).
  For example: Qpole gradients, *QP_G*.

During the linac design and construction phases, links between real and virtual parameters were estimated, with a certain degree of confidence considered as sufficient to initiate the construction of the machine (with considered margins).

For example: $QP\_G = k0\ [\pm dk] \times QP\_I$

Bayesian Improvement of the DT

During the linac lifetime, starting with commissioning, we propose to adjust gradually, experiment after experiment, the links between real and virtual parameters to improve the DT using a Bayesian inference technics [6]. In order to do this, one needs the following abilities:

- Be able to store in a database each experimental result, their uncertainties and associated machine configuration (installed devices and control parameters).
- Be able to simulate the best as possible the results of the experiments (having a DT).

ISBN: 978-3-95450-253-0 ISSN: 2673-5571 doi:10.18429/JACoW-HB2023-TUA3I4

- Be able to calculate a "distance" between experimental and simulated measurements.
- Be able to figure out the DT parameters minimizing the average weighted distance of all experiments and associated uncertainties.

The Bayesian method is the following:

Considering A, a set of experimental measurements and B, a set of parameters in the DT, Bayes formula gives:

$$p(B/A) = \frac{p(A/B)}{p(A)} \times p(B)$$

- $p(B/A)$ is the probability of a set DT parameters after the experiments,
- $p(A/B)$ is the simulation by the DT of the experimental results,
- $p(A)$ is the uncertainties on the experimental measurement (error bar),
- $p(B)$ is the probability of the DT parameters before the experiments.

The best set of DT parameters B_{opt} are those maximising $p(B/A)$ or can also be given by: $B_{opt} = \frac{\int p(B/A)\times B\cdot dB}{\int p(B/A)\cdot dB}$.

The uncertainties of the DT parameters are given by the variance matrix: $V_B = \frac{\int p(B/A)\times B\times B^{*}\cdot dB}{\int p(B/A)\cdot dB}$.

This global evaluation (considering all experimental results at once) can be replaced by an incremental one, which can be improved after each (set of) experiment(s) A_n:

$$p(B/A_n) = \frac{p(A_n/B)}{p(A_n)} \times p(B/A_{n-1})$$

$$p(B/A_n) = \prod_{i=1}^{n} \frac{p(A_i/B)}{p(A_i)} \times p_0(B)$$

- The DT parameters can then be « adjusted » experiment after experiment.
- If needed, all the experiments can be processed again from time to time (in case of re-evaluation of some data).
- New parameters can be added in the DT without losing what has been learned on other parameters.
- Analysing deviant experimental results can help to:
  - Either improve measurement understanding (badly simulated, experimental errors),
  - or improve linac model (missing parameters),

Simulation of Bunch Length Measurement

One the necessary tools is to implement in the DT the best simulation as possible of the experimental measurement.

On bunch length measurement, we them implemented:

- The sampling by the FFC of only a 0.5 mm transverse sample of the beam,
- The "bounce" of the signal (integration part),
- The 6 GHz bandwidth of the scope.

Figure 12 shows that implementing these experimental conditions have a non-negligible impact on the datas extracted from the measurement.

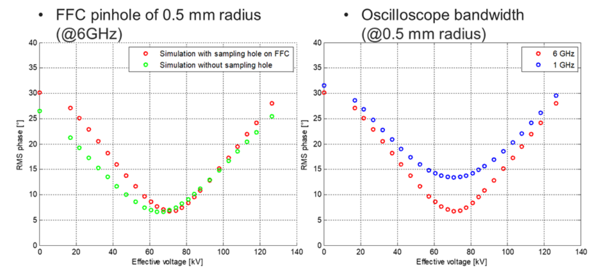

Figure 12: Impact of the DT measurement simulation on the experiment results. Left, integrated pinhole configuration; Right, integrated oscilloscope bandwidth.

Once the DT is able to simulate the experiment, one can compare directly their results, evaluate a distance between them (either on profiles or on RMS sizes, FWHM…) and find-out the DT parameters that minimize it. Fig. 1 shows a global comparisons between the experimental results and the present DT evaluations.

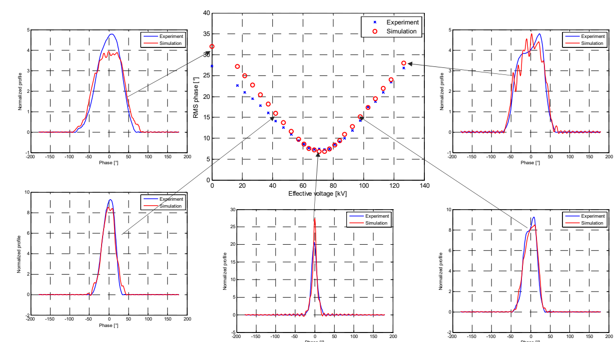

Figure 13: Comparisons between experimental and DT simulation profiles and sizes.

Before conclusion, here is a little story illustrating the power of the method:

When doing the transverse emittance measurements (Quad scan) of the 5 mA proton beam, one remarked that the experiment results were very different from the DT predictions.

Strategy 1: we could have kept the experiment result "as reality" and have considered that the beam transverse parameters were not "as expected", trying to implement them in the code.

Strategy 2: Nevertheless, using this "machine learning" philosophy, we observed that the experimental results were much better reproduced by considering an increasing of the focusing force by about +20% (much more that estimated initial uncertainties of a few %).

Finally, checking the Control-System configuration, one found out that there was a mistake on the G_QP/I_QP parameter by +18% (wrong magnetic length was used)!

By using strategy 1, one would have resolved the incoherence between code and measurement by compensating two errors (on the initial distribution AND in Qpole gradi-

ISBN: 978-3-95450-253-0 ISSN: 2673-5571 doi:10.18429/JACoW-HB2023-TUA3I4

ents). Nevertheless, this would have produced new incoherences with other MEBT configurations (deuterons, current…).

Using strategy 2 allowed us to improve our machine knowledge for all configurations, even those not tested.

CONCLUSION

The MEBT was installed at SARAF, followed by its commissioning with and without beam. The feasibility of transporting 5 mA proton and deuteron beams was demonstrated and the main characteristics were analysed.

A new way to process the experimental data have started, consisting of coupling the real machine with its Digital Twin whose parameters can be adjusted from experimental results. A lot of tools have still to be implemented for this, but the first results look promising.

The activities on SARAF will continue finally the installation and commissioning of the cryomodules.

REFERENCES

[1] N. Pichoff *et al.*, "The SARAF-linac project status", in *Proc. IPAC'23*, Venice, Italy, May 2023, pp. 2313-2315. doi:10.18429/JACoW-IPAC2023-TUPM053

[2] J. Rodnitski, private communication.

[3] D. Uriot and N. Pichoff, "Status of TraceWin code", in *Proc. IPAC'15*, Richmond, VA, USA, pp. 92-94. doi:10.18429/JACoW-IPAC2015-MOPWA008

[4] T.L. Owens *et al.,* "Phase scan signature matching for LINAC tuning", in *Proc. LINAC'94*, Tsukuba, Japan, Aug. 2014, paper TH-80, pp. 893-895.

[5] L. Weissman *et al.,* "SARAF linac: status on 2023", Unkel, Germany, Sep. 2023, submitted for publication.

[6] See for example, https://en.wikipedia.org/wiki/Bayesian_inference